

# Observations about the Seismic Response of RC Buildings in Mexico City

**Sergio Alcocer,<sup>1</sup> Anahid Behrouzi,<sup>2</sup> M. EERI, Sergio Brena,<sup>3</sup> M. EERI Ken Elwood,<sup>4</sup> M. EERI Ayhan Irfanoglu,<sup>5</sup> M. EERI Michael Kreger,<sup>6</sup> M. EERI Remy Lequesne,<sup>7</sup> M. EERI Gilberto Mosqueda,<sup>8</sup> M. EERI Santiago Pujol,<sup>9</sup> M. EERI Aishwarya Puranam,<sup>10</sup> M. EERI Mario Rodriguez,<sup>11</sup> M. EERI Prateek Shah,<sup>12</sup> M. EERI Andreas Stavridis,<sup>13</sup> M. EERI and Richard Wood<sup>14</sup> M. EERI.**

Over 2000 buildings were surveyed by members of the Colegio de Ingenieros (CICM) and Sociedad Mexicana de Ingenieria Estructural (SMIE) in Mexico City following the Puebla-Morelos Earthquake of 2017. This inventory of surveyed buildings included 40 collapses and over 600 buildings deemed to have structural damage. Correlation of damage with peak ground acceleration (PGA), peak ground velocity (PGV), predominant spectral period, building location, and building properties including height, estimated stiffness, and presence of walls or retrofits was investigated for the surveyed buildings. The evidence available suggests that: 1) ground motion intensity (PGV) and not ground motion predominant period drove the occurrence of damage, and 2) buildings with more infill and stiff retrofit systems did better than other buildings.

---

<sup>1</sup> University of Texas San Antonio, One UTSA Circle San Antonio, TX 78249.

<sup>2</sup> Cal Poly San Luis Obispo, 1 Grand Avenue, San Luis Obispo, CA 93407

<sup>3</sup> University of Massachusetts Amherst, 130 Natural Resources Road, Amherst, Massachusetts 01003

<sup>4</sup> University of Auckland, 314 Khyber Pass Rd, Auckland, 1010

<sup>5</sup> Purdue University, 1040 S River Rd., West Lafayette, IN, 47907

<sup>6</sup> University of Alabama, 401 7<sup>th</sup> Avenue, Tuscaloosa, AL 35401

<sup>7</sup> University of Kansas, 2150 Learned Hall, 1530 W. 15<sup>th</sup> St, Lawrence, KS 66045

<sup>8</sup> University of California San Diego, Voight Drive, La Jolla, CA 92093

<sup>9</sup> Purdue University, 1040 S River Rd., West Lafayette, IN, 47907

<sup>10</sup> National Taiwan University, No.1, Sec. 4, Roosevelt Road, Taipei, 106 Taiwan

<sup>11</sup> Universidad Nacional Autonoma de Mexico, Ciudad Universitaria, Coyoacan México D.F., C.P. 04510

<sup>12</sup> Purdue University, 1040 S River Rd., West Lafayette, IN, 47907

<sup>13</sup> University at Buffalo, 224 Ketter Hall, Buffalo, NY 14260

<sup>14</sup> University of Nebraska-Lincoln, 362 K Whittier Research Facility, 2200 Vine St., Lincoln, NE 68588

## INTRODUCTION

The Puebla-Morelos (or Central Mexico) Earthquake occurred on 19 September 2017 and had a moment magnitude of 7.1 (USGS 2017, SSN 2017). The Colegio de Ingenieros of Mexico City (CICM) and Sociedad Mexicana de Ingenieria Estructural (SMIE) organized a survey following the earthquake to assess damage and to collect information and identify buildings that posed a risk to occupants and therefore required evacuation. Approximately 35 teams visited the most affected areas of the city and surveyed nearly 2,000 buildings (CICM and SMIE 2017). The teams were composed of civil engineers and civil engineering students and each team was led by an experienced structural engineer. Teams were assigned sections of the city to survey and members walked throughout their assigned sections and randomly selected structures to be surveyed. Engineers attempted to enter each structure to survey the interior of the building. Observations of damage were noted on a standardized form. Information collected by the survey teams was sent back to CICM where it was collected and organized into a spreadsheet along with photographs. Well-trained structural engineers along with experienced researchers from local universities carefully reviewed the field data to identify and flag errors related to damage classification. Teams were sent back to the field to correct errors. The engineers also collected: (1) information about geotechnical zoning in the city with help from the Sociedad Mexicana de Ingenieria Geotecnica (SMIG), and (2) ground motion records from 61 stations across the city made available by the Centro de Instrumentacion y Registro Sismico C.A. (CIRES) and National Autonomous University of Mexico (UNAM). Locations of surveyed buildings and stations for recording ground motions are shown in **Fig. 1** superimposed on geotechnical zones.

**Figure 1.** Locations of buildings surveyed by CICM and SMIE and CIRES accelerometers superimposed on maps of geotechnical zones (CICM and SMIE, 2017)

Data collected and shared by CICM and SMIE included building properties such as location, number of stories, and use, as well as the type of damage observed at each location. The data indicate for each surveyed structure whether team members observed collapse, partial collapse, damage to structural elements (beams, columns, or walls), damage to non-structural elements, inclination, or differential settlement. Throughout this manuscript, the term collapse is used to refer to the complete loss of elevation of one or more stories (**Fig. 2**). All structures identified by CICM and SMIE (2017) as having collapsed were verified by the writers in person during

subsequent surveys or via news reports. Structures identified by CICM and SMIE as exhibiting partial collapse were omitted from this study because the definition was less clear. In relation to the survey done by CICM and SMIE, the term damage is used herein to refer to instances of “structural damage” where one or more structural elements exhibited clear signs of distress caused by shear, bond, or axial stresses (**Fig. 3**). Buildings with damage to only non-structural elements are not included among damaged buildings considered in this paper.

**Figure 2.** Examples of collapses in buildings surveyed by CICM and SMIE (2017)

**Figure 3.** Examples of structural damage in buildings surveyed by CICM and SMIE (2017)

A team of researchers from universities in the United States, Mexico, and New Zealand (the writers) subsequently surveyed approximately 110 buildings and instrumented 13 buildings to measure fundamental period. All data collected are available at <https://datacenterhub.org/resources/14746>. These additional surveys provided detailed data regarding the type and extent of damage observed. Each structure was assigned a damage index that ranged from 1 for little or no structural damage to 10 for structures with partial or complete collapse or failure of structural members. This survey also recorded information about the structural systems, including the presence of retrofits and the cross-sectional area and orientation of reinforced concrete columns and walls as well as masonry infill walls. Buildings were selected following these criteria: a) location (buildings were surveyed in the areas illustrated in **Fig. 1** with preference for areas where damage indicated higher intensity), b) inclusion of both buildings with and without damage in areas investigated, and c) accessibility and disruption of use. Most undamaged buildings included in this survey were located near surveyed damaged buildings and appeared to be similar in proportions and vintage to surveyed damaged buildings.

This article reflects on some of the observations made after the 1985 Michoacán Earthquake and uses data available from 2017 to investigate the correlation of structural damage and collapse with building properties, ground motion intensity, and geotechnical conditions. The list of building properties studied is provided in Appendices A and B. Appendix A refers to properties collected and studied by the writers. They follow (in format and content) from previous investigations by Shiga et al. (1968), Riddell et al. (1987), Hassan and Sozen (1997), Dönmez and Pujol (2005), O'Brien et al. (2011), Islam et al. (2017), Pujol et al. (2019). Appendix B lists information collected by CICM that is described at <https://www.sismosmexico.org/informes>. Considered ground motion

characteristics included peak ground acceleration (PGA), peak ground velocity (PGV), and the predominant ground motion period, defined as the period associated with the maximum spectral displacement for a linear system because of the properties of the site and their effects on response. Geotechnical conditions were considered qualitatively by correlating the locations of damaged buildings with geotechnical zones.

## ANALYSIS

### **Background: 19 September 1985 Michoacán Earthquake (M 8.1, USGS 1985)**

In the 1985 Michoacán Earthquake, the majority of collapses in Mexico City occurred for buildings with 6 to 10 stories (**Fig. 4**), although the majority of the buildings in the city had 5 or fewer stories (Aguilar et al., 1989). Detailed information about this set of buildings was summarized by Aguilar et al. (1989) and these data have been used by a number of researchers to study the response of buildings to the 1985 Michoacán Earthquake (Stone et al. 1985, NZSEE 1985, Aguilar et al. 1989, Teran-Gilmore and Bertero 1992).

**Figure 4.** Reinforced concrete buildings with severe structural damage and partial or complete collapse, Mexico City, 1985 (Reproduced using data from Aguilar et al. 1989)

Only a limited number of ground motions were recorded within the city during the 1985 event. The record from Station SCT (located halfway between rock and the deepest soil deposits on the west side of the city, **Fig. 5a**) produced the linear-elastic and nonlinear (elastic-plastic) displacement spectra for single-degree-of-freedom (SDOF) oscillators shown in **Fig. 5b**. The linear-elastic displacement spectrum has large amplifications between 1.5 s and 3.5 s. The consensus of the profession seemed to be that the large amplifications in this range explained the relatively large number of damaged and collapsed buildings with 6 to 10 stories. The stiffness of the soils, distance from the source, focal mechanism and magnitude of the earthquake have been suspected to have produced this concentration of demand and damage in taller buildings (Stone et al. 1985, NZSEE 1985, Aguilar et al. 1989).

An issue that may have received less attention is that spectra with narrow bands of large amplification do not affect nonlinear systems the same way they affect linear systems (Pujol et al., 2018). Large amplifications in narrow period ranges resemble the phenomenon of resonance. Nonlinear structures are not prone to resonance because their stiffness changes from one instant to

the next during strong ground motion. Most of the structures affected by the earthquake of 1985, however, were flexible and brittle structures with limited ability to retain their structural integrity during displacement cycles applied after they reached their lateral strength. It seems reasonable to believe that, after initial softening caused by cracking, their response depended on the magnitude of linear demands at elongated periods and increased damping. In that scenario, the range of periods with large amplifications in linear structures would be critical in the retrofit or evaluation of such brittle structures. Nevertheless, this range is likely to be less critical for ductile nonlinear structures.

**Figure 5.** (a) Location of station SCT and zone of severe damage in 1985 (using data from Stone et al 1987), and (b) displacement spectra for SDOF linear and nonlinear oscillators to the E-W component of the 1985 earthquake recorded at the SCT station (damping ratio = 5%).

#### **2017: 19 September Puebla-Morelos Earthquake (M 7.1, USGS 2017)**

Buildings surveyed by CICM and SMIE after the 2017 Puebla-Morelos Earthquake are located in **Figs. 6 and 7**. It is interesting that relative to the observations from 1985, in 2017: 1) the reported structural damage seems to have shifted towards shorter buildings, 2) more buildings were reported damaged, and 3) fewer collapses occurred. **Fig. 7** illustrates that the correlation between damage and building height was not clear in 2017. In general, the distribution of damage is shifted towards buildings with 5 or fewer stories, which, by inspection, is the most prevalent class of buildings in Mexico City. The distribution of damage therefore reflected to some extent the distribution of buildings in the city. The CICM-SMIE survey reported 40 collapses in the 19 September 2017 Earthquake. Although 10 of these 40 collapses occurred in buildings with 5 stories, the concentration of collapse occurrence in buildings within a given height range (**Fig. 8**) was not as clear as in 1985 (**Fig. 4**).

**Figure 6.** Locations of damaged and collapsed buildings after 2017 Puebla-Morelos Earthquake

**Figure 7.** Buildings surveyed after 2017 Puebla-Morelos Earthquake (data from CICM and SMIE, 2017) – Note the use of two different vertical scales.

**Figure 8.** Height, in terms of number of stories, of collapsed buildings in Mexico City, 2017 Puebla-Morelos Earthquake

### Frequency of Damage vs. Building Height

Correlation between damage and building height was also investigated by estimating frequency of damage for different ranges of building heights. Frequency of damage is defined as the number of buildings classified as having structural damage or collapse divided by the number of buildings inspected (as opposed to total number of buildings) for each range of building height. This definition was used because the authors do not have an accurate count of buildings in Mexico City and because it would not make sense to mix in buildings from areas where shaking had low intensity. Realize that this definition of frequency results in values much larger than the actual frequency of damage in the entire city because the number of inspected buildings (the denominator) is much smaller than the total number of buildings in Mexico City. In the results from the CICM-SMIE survey, the frequency of damage seems to have been uniform across a wide range of building heights below 15 stories (**Fig. 9**) i.e. no concentration of damage is seen for any particular range of building height. The same is true even if one ignores 1- and 2-story buildings (**Fig. 9**), which are often confined masonry structures in Mexico City, while taller buildings tend to be RC frames with masonry infill. While it is not known how survey methods may have influenced the calculated frequency of damage, it is clear that many buildings with fewer than 6 stories ( $N < 6$ ) were damaged (**Fig. 7**). Nevertheless, engineers interviewed by the writers suggested that most of the damaged buildings had 6 to 8 stories which was a new occurrence of “resonance” similar to that reported in 1985 (a view that dominates design in Mexico City). This interpretation is inconsistent with the data plotted in **Fig. 9**.

**Figure 9.** Frequency of damage vs. number of stories in 2017

### Frequency Content of Ground Motion

A network of accelerometers maintained by CIRES and UNAM produced 61 records from Mexico City during the September 19, 2017 Earthquake. **Fig. 10** shows the locations of these accelerometers.

**Figure 10.** Locations of CIRES and UNAM accelerometers in Mexico City (2017)

The damage distribution observed in 2017, which in relative terms included more buildings with fewer than 6 stories, could also be interpreted as the result of larger demands at shorter periods (higher frequencies) in relation to the ground motions in 1985. That was indeed the case at station

Ciudad Universitaria (CU), located on rock, and for periods shorter than 0.5s (or frequencies exceeding 2Hz) (**Fig. 11a**). Nevertheless, in that area, intensity was relatively small and damage was not frequent. In contrast, the ground motions recorded on soil both at station SCT and in the area where most damage occurred (Condesa and Roma districts) show that demands in 2017 were not always higher for shorter periods (higher frequencies) (**Fig. 11b and c**). The records show linear spectral accelerations and displacements for periods of up to 1.75s were similar in 1985 and 2017. On the other hand, demands for longer periods (lower frequencies) were much smaller in 2017. That observation is consistent with the relative reduction in damage to taller structures.

**Figure 11.** Spectral displacements and accelerations for the 1985 and 2017 ground motion records (damping ratio = 5%)

But how can one then explain the damage in shorter structures that had already survived the motion of 1985 which was at least as demanding as the 2017 motion? Many factors may be at play here. One may be accumulation of damage. Another factor may be that the building inventory aged and may have been altered by remodeling. But other factors are:

- 1) The variability of ground motion intensity across the city. There were locations in which nearly no signs of intense ground motion were observed with occupants reporting no damage to contents whatsoever. Nevertheless, just a few blocks away, numerous collapses occurred. Unfortunately, accelerometers were too sparsely distributed to provide a comprehensive record of how ground motion intensity varied from block to block (admittedly a difficult task), and how the distribution differed from the 1985 earthquake.
- 2) The brittleness of the structures. In a brittle and flexible structure, a small change in demand may lead to a large change in response. Flexibility here refers to the inverse of stiffness and not to deformability.
- 3) All of the mentioned factors combined.

Another interesting question is why the 2017 motion was weaker for long periods (i.e. low frequencies)? There is no clear answer, but factors to be considered include:

- Difference between attenuation of long period and short period waves
- Whether soils have changed over time because of drainage

Geotechnical zones (dominant spectral period) and building period

The experience of 1985 created a lasting impression among engineers in Mexico and also led to a change in seismic zonation in the City (Iglesias, 1989). Conversations with design professionals in Mexico City indicated their designs are often aimed at avoiding “resonance.” In 2017, most damage occurred in a narrow geographic “band” running N-S that encompasses three geotechnical (or seismic) “zones” II, IIIa and IIIb between rock and the old lakebed as illustrated in **Fig. 6**. Most collapses (black dots in **Fig. 6** occurred in a zone classified according to its soil as “Zone IIIa” (in orange).

Given the precedent from 1985, the question now is whether the damage and collapses occurred in Zones II, IIIa and IIIb because the periods of the soils matched the periods of the affected buildings. To address this question, linear displacement response spectra were produced from the acceleration records at station locations shown in **Fig 10**. From these spectra, the period producing the highest linear displacement demand was obtained and named “dominant spectral period.” If the problem of earthquake demand in Mexico City is one of resonance, then one should expect the ratio of building period to dominant spectral period to help organize observations related to instances of damage.

The plots in **Fig. 12** are attempts to evaluate the idea that resonance explains which buildings experienced more damage in Mexico City during the earthquake of 2017. The vertical axis is percent of surveyed buildings classified as having structural damage and as in **Fig. 9**, this represents frequency of damage for the collected sample of data and not the actual frequency of damage for the entire city. The horizontal axis is the ratio of estimated building period (taken as number of stories (N)/8) to dominant spectral period from the record closest to that building. Stark (1988) reported periods (T) larger than N/8 for reinforced concrete structures from measurements made after the 1985 earthquake in Mexico City. Here, N/8 is assumed to be a reasonable estimate of fundamental period of common RC frames in Mexico City and this assumption is supported by data described in the next section. This assumption was also made considering that in Mexico City masonry infills stiffen buildings producing shorter periods but often in a single direction of the floor plan as discussed later.

**Figure 12.** Correlation between frequency of damage and dominant spectral period for all buildings (left) and buildings with  $N > 2$  (right)

**Fig. 12** suggests that the analogy of resonance was not as useful in 2017 as it may have been in 1985. But one aspect is clear in this trend: stiffer buildings founded on softer soils (represented by the 0-0.5 range on the chart) had less damage. That is evident also from the absence of damage in the Eastern parts of the city, in the old lake area with deeper and longer period soil deposits, where most structures are 1 and 2-story confined masonry houses. These structures were spared as were most stiff buildings in the center of the Kathmandu valley during the Gorkha Earthquake in Nepal in 2015 (Shah et al., 2017).

### Instrumenting Structures to Estimate Period

To test the idea that period is close to  $N/8$  for a typical RC frame in Mexico City (with 3 to 15 stories), the writers instrumented a number of structures in early 2018 to collect ambient vibration data with the following understanding:

1. period is sensitive to amplitude of oscillations
2. buildings instrumented were likely to have been stiffer before the earthquakes that affected them
3. we were unlikely to obtain a truly representative sample without investing large resources
4. interaction with adjacent structures and soils make the process difficult
5. period identification is not always unequivocal

With these shortcomings in mind, we identified the longest periods of vibration for each floor-plan direction in 13 buildings having RC frames with masonry infills.

### **Figure 13.** Longest periods of vibration inferred from ambient vibrations

The data in **Fig. 13** were obtained with two separate sets of instruments (represented with filled and open circles), and different data processing methods, and spectra used to identify periods. The spread of the data and differences between systems / processes show that the use of ambient vibrations to estimate the period for the selected buildings was far from crisp. Yet, two trends seem consistent:

1. Except for corner buildings, in the direction perpendicular to the street, buildings had long and continuous infill walls (often made with brick) that provided substantial stiffness. In this direction, the period was approximately  $N/12$  after the earthquake.

2. In the direction of the street, buildings had few and mostly discontinuous and perforated infill walls that did not provide as much additional stiffness to RC frames. In this direction, the period was approximately  $N/8$  after the earthquake.

It follows that assuming the period as being close to  $N/8$  or shorter in the weak direction (that of the street), is reasonable. It also follows that the corner buildings are more vulnerable to drift and prone to torsion, making for compounded vulnerability. Indeed, as pointed out in the report by CICM and SMIE (2017), approximately 50% of collapses occurred in corner buildings, and by inspection the percent of corner buildings in the city building stock is much lower than 50%.

### Ground Motion Intensity

The resonance analogy may not apply in the case of 2017 simply because ground motion intensity seems to have had sharp variations within the city. Observations from the field made this evident: as mentioned, some areas of the city had heavy damage while other areas with buildings of similar vintage and height did not. The implication is that the occurrence of damage was not solely a function of period and soil type and may also be influenced by basin or other effects.

To try to understand better the distribution of damage, a contour map of ground motion intensity (**Fig. 14**) was produced using values of peak ground velocity (PGV) obtained from acceleration records published by CIRES. PGV has been reported to correlate well with drift demand (Sozen 2003, and Laughery 2016).

**Figure 14.** Contour of PGV (purple represents low PGV ( $\sim 10\text{cm/s}$ ) and red represents high PGV ( $\sim 50\text{cm/s}$ ), and black dots represent collapsed buildings)

The contour map includes dots representing locations of building collapses. At first glance, it appears as if collapse locations match locations with higher values of PGV. But a closer look reveals that a number of collapses occurred in areas with lower PGV on the West side of the city, and large areas with large values of PGV on the East side had no collapses.

The variation of PGV across a swath of the city (bounded by the horizontal lines in **Fig. 14** representing latitudes of 19.35 and 19.45 degrees) is illustrated by the profile in **Fig. 15**.

**Figure 15.** Variation of PGV from West to East between latitudes 19.35 and 19.45 degrees

The low intensities on the West are attributed to the presence of rock and shallow soil deposits. The high intensities on the East could be attributed to deep soil deposits from the original lakebed and basin effects. But the fluctuations in the center are not as easy to attribute to the properties of the soils indicated by the soils map in **Fig. 6**.

Driving through the city reveals that taller buildings are concentrated along a rather narrow corridor running nearly N-S near the West edge of the city. Detailed information on density of buildings and building heights is not available to the writers. But we do have the information on building height (number of stories) collected by CICM-SMIE for nearly 2000 buildings. The average number of stories for all surveyed buildings in the swath depicted in **Fig. 14** is shown in the profile in **Fig. 16**. Most of these surveyed buildings had fewer than 20 stories.

**Figure 16.** Variation of building height from West to East

**Fig. 16** can be thought of as a city “profile.” Near the East and West boundaries of the plot, no information was available but an average height of 1.5 stories, inferred from photographs published by Google, is used. The plot confirms the impression described above that buildings with more than 2 stories concentrate on a 5-km band between longitudes 99.2W and 99.1W deg. Given that short 1 to 2-story houses are typically confined-masonry structures while taller buildings tend to have flexible (at least in one direction) RC frames, it should not be surprising that the two different types of structures had different performance. We chose to focus on those with frames.

Assuming that building average height is an indicator of the density of RC frames in the city, comparing **Figs. 15** and **16** would suggest that there was an area in which both demand and RC-frame density were high. West of -99.2 degrees longitude, both the demand and density were low. East of -99.1 degrees longitude, demand was high but RC frames are sparse. In contrast, near the meridian at 99.15W, both demand and building density were high. This can be illustrated by multiplying PGV (normalized relative to 40 cm/s) and number of stories (normalized relative to 8) to obtain this new profile combining both demand and building density (**Fig. 17**).

**Figure 17.** Variation of drift demand and collapsed buildings

The number of collapses and damaged buildings near a given meridian is superimposed on the plot in **Fig. 17** to show that damage concentrated where two rather obvious (in retrospect) factors

coincided: RC frame buildings (as opposed to one or two story masonry houses) and high ground motion intensity (PGV). This figure also implies that matching soil and building period may be less important. **Fig. 17** emphasizes indirectly the relevance of drift demand because, as stated above, PGV has been reported to correlate well with drift demand.

Two more sets of plots confirm the observations above about the importance of intensity and fundamental period (as a measure of stiffness and mass). **Fig. 18** shows that damage frequency among the surveyed buildings increased with both PGV and PGA. Incidentally, reexamining the effect on damage frequency of the ratio of building period to dominant spectral period to focus on only areas with high PGV did not produce better correlation than obtained for the entire dataset.

**Figure 18.** Frequency of damage in buildings with  $N > 2$  vs. PGV and PGA

Note: Both plots exclude buildings close to stations that recorded  $PGV < 10$  cm/s.

**Fig. 19** shows the mean damage index assigned by the authors based on data collected on-site plotted versus wall density (measured as the ratio of cross-sectional area of infill wall<sup>15</sup> to floor plan area). The damage index was chosen to be 1 for little or no structural damage, 5 for moderate damage, and 10 for building collapse and structural failures (Appendix A). **Fig. 19** shows that the buildings with larger wall densities performed better despite the modest drift capacity of infill. If said capacity is exceeded-of course- the apparent benefits of the infill can be compromised and the bare frame may see increased deformation demands and column shear forces where infills fail. In addition, it was clear that buildings retrofitted following the 1985 event by adding stiffening elements (often RC infill walls) performed quite well in 2017 (Roselin et al., 2019).

**Figure 19.** Average damage index vs. wall density

Note: Data used to produce this plot are available at <https://datacenterhub.org/resources/14746> and Design Safe (PRJ-1800 and PRJ-2285).

## CONCLUSIONS

---

<sup>15</sup> Most walls were masonry infill. RC walls were present in isolated cases. They were treated as being equivalent to produce Figure 19.

1. Damage concentrated where two rather obvious (in retrospect) factors coincided: RC frame buildings (as opposed to one or two story masonry houses) and high ground motion intensity (PGV).
2. The ratio of building period to predominant ground motion period did not have a strong correlation with damage frequency.
3. The evidence available suggests that ground motion intensity (PGV and PGA) and not predominant ground motion period drove the occurrence of damage. It also suggests that stiffer buildings performed better.
4. Buildings with more infill walls and stiff retrofit systems performed better than other buildings.

## ACKNOWLEDGEMENTS

This work was supported by The National Science Foundation (Award 1810870). The authors would like to thank the Colegio de Ingenieros de Ciudad de México (CICM) and Sociedad Mexicana de Ingeniería Estructural (SMIE) for generously sharing the collected data and for supporting our reconnaissance activities in Mexico City. The authors also gratefully acknowledge the following people and organizations for their support.

Luciano Fernández, UAM

David Muria Vila, UNAM

Hugón Juarez, UAM

Rajesh Dhakal, University of Canterbury

García Jarque Ingenieros

Rodolfo Valles, WSP Group

Antonio Sandoval

Nancy Ariceaga

Roberto Stark

U.S. National Science Foundation, NSF

American Concrete Institute, ACI

New Zealand Society for Earthquake Engineering, NZSEE

Instituto Nacional de la Infraestructura Física Educativa, INIFED

## REFERENCES

Aguilar, J., Juarez, H., Ortega, R., and Iglesias, J., 1989. The Mexico Earthquake of September 19, 1985—Statistics of Damage and of Retrofitting Techniques in Reinforced Concrete Buildings Affected by the 1985 Earthquake. *Earthquake Spectra*, Vol. 5, No. 1.

Colegio de Ingenieros Civiles de México (CICM), Sociedad Mexicana de Ingeniería Estructural (SMIE), 2017. Information about the earthquake of September 19 2017 available at [http://www.cires.org.mx/racm\\_mapa/index.php](http://www.cires.org.mx/racm_mapa/index.php) (last accessed October 1 2018).

Colegio de Ingenieros Civiles de México (CICM), Sociedad Mexicana de Ingeniería Estructural (SMIE), 2017. Resumen Preliminar de Daños de Los Inmuebles Inspeccionados por Las Brigadas del CICM del SISMO del 19/09/2017. Report available at [http://www.cires.org.mx/racm\\_mapa/index.php](http://www.cires.org.mx/racm_mapa/index.php) (last accessed October 1 2018).

Dönmez, C. and Pujol, S., 2005. Spatial Distribution of Damage Caused by the 1999 Earthquakes in Turkey. *Earthquake Spectra* - EARTHQ SPECTRA. 21. 10.1193/1.1850527.

Hassan, A., and Sozen, M., 1997. Seismic vulnerability assessment of low-rise buildings in regions with infrequent earthquakes. *ACI Structural Journal*. 94(1):31–39

Iglesias, J. 1989. The Mexico Earthquake of September 19, 1985- Seismic Zoning of Mexico City after the 1985 Earthquake. *Earthquake Spectra*, Vol. 5, No. 1, pp 273-291.

Islam, M.S., Alwashali, H., Torihata, Y., Jin, K., Maeda, M., 2017. Rapid seismic capacity evaluation method of RC buildings with masonry infill. *Architectural Institute of Japan-Academic Lecture Collection Summary*. pp 195–196, August.

Laughery, L., 2016. Response of High-Strength Steel Reinforced Concrete Structures to Simulated Earthquakes. Ph.D. Thesis, Purdue University, West Lafayette, IN.

New Zealand Society of Earthquake Engineering (NZSEE), 1988. The September 1985 Mexico Earthquakes: Final Report of the New Zealand Reconnaissance Team. *Bulletin of the New Zealand Society for Earthquake Engineering*, Vol. 21, No.1, March 1988

O'Brien, P., Eberhard, M., Haraldsson, O., Irfanoglu, A., Lattanzi, D., Lauer, S., Pujol, S. 2011. Measures of the seismic vulnerability of reinforced concrete buildings in Haiti. *Earthquake Spectra* 27(S1): S67–S92

Olsen, A., Aagaard, B., Heaton, T., 2008. Long-Period Building Response to Earthquakes in the San Francisco Bay Area. *Bulletin of the Seismological Society of America*, Vol. 98, No. 2.

Pujol, S., Irfanoglu, A., Gulkan, P., Heaton, T.H., Sozen, M.A., and Laughery, L., 2018. A Potential Problem in Estimating the Drift Response of Long-Period Structures. *Proceedings of the 11th U.S. National Conference on Earthquake Engineering*. Los Angeles, California.

Pujol, S., Laughery, L., Puranam, A., Hesam, P., Cheng, L-H., Lund, A., Irfanoglu, I., 2019. Evaluation of Seismic Vulnerability Indices Including Data from the 6 February 2016 Taiwan Earthquake. *Journal of Disaster Research*, 14(4).

Riddell, R., Wood, S.L., de la Llera, J., 1987. The 1985 Chile Earthquake; Structural Characteristics and Damage Statistics for the Building Inventory in Viña del Mar. *Civil*

*Engineering Studies, Structural Research Series No. 534*, University of Illinois, Urbana, August 1987, 265 pp.

Roselin, S., Juarez-Garcia, H., Dhakal, R.P., Gomez-Bernal, A., 2019. The September 19<sup>th</sup>, 2017 Puebla, Mexico Earthquake: Final Report of The New Zealand Reconnaissance Team. Draft submitted to the *Bulletin of the New Zealand Society for Earthquake Engineering*.

Servicio Sismologico Nacional (SSN), 2017. Special Report on the 19 September 2017 Puebla Morelos Earthquake available at <https://www.sismosmexico.org/informes> (last accessed October 1 2018)

Shah, P., Pujol, S., Kreger, M., McCabe, S., Irfanoglu, A., 2017. 2015 Nepal Earthquake, Damage Assessment Survey. *Concrete International*, Vol. 39, No. 3.

Shiga, T., Shibata, A., Takahashi, T., 1968. Earthquake damage and wall index of reinforced concrete buildings. *Proceedings of the Tohoku district symposium*. Architectural Institute of Japan, no. 12, Dec. 1968, pp 29–32 (in Japanese)

Sozen M.A., 2003. The Velocity of Displacement. In: *Wasti S.T., Ozcebe G. (eds) Seismic Assessment and Rehabilitation of Existing Buildings. NATO Science Series (Series IV: Earth and Environmental Sciences)*, Vol 29. Springer, Dordrecht.

Stark, R., 1988. Evaluation of Strength, Stiffness and Ductility Requirements of Reinforced Concrete Structures using data from Chile (1985) and Michoacán (1985) Earthquakes. Ph.D. Thesis, University of Illinois at Urbana-Champaign, Illinois.

Stone, W.C., Yokel, F.Y., Celebi, M., Hanks, T., and Leyendecker, E.V., 1987. Engineering aspects of the September 19, 1985 Mexico Earthquake. *National Bureau of Standards Science Series*, 165.

Teran-Gilmore A., Bertero, V., 1992. Performance of Tall Buildings During The 1985 Mexico Earthquakes. Earthquake Engineering Research Center, Report No. UCB/EERC-92/17.

United States Geological Survey (USGS), 1985. M 8.0 - Michoacán, México. Available at <https://earthquake.usgs.gov/earthquakes/eventpage/usp0002jwe#executive>. [last accessed October 1 2017].

– FINAL DRAFT –

Published version available at: <https://doi.org/10.1177/8755293020942523>

United States Geological Survey (USGS), 2017. M 7.1 – 1km E of Ayutla, Mexico. Available at <https://earthquake.usgs.gov/earthquakes/eventpage/us2000ar20/executive>. (last accessed October 1 2017).

## APPENDIX A

List of parameters obtained for each building surveyed by writers  
([https://datacenterhub.org/dv\\_dibbs/view/1723](https://datacenterhub.org/dv_dibbs/view/1723)):

Number of Stories Above Ground

Number of Stories Below Ground

Year of Construction

Structural System

First Floor Height [cm]

Typical Exterior Column Width [cm]

Typical Exterior Column Breadth [cm]

Typical Interior Column Width [cm]

Typical Interior Column Breadth [cm]

Typical NS/Parallel Span [cm]

Typical EW/Perpendicular Span [cm]

Masonry Wall Thickness [cm]

RC Wall Thickness [cm]

Column Area Ratio [%]

NS/Street Parallel Masonry Wall Ratio [%]

EW/Street Perpendicular Masonry Wall Ratio [%]

NS/Street Parallel RC Wall Ratio [%]

EW/Perpendicular RC Wall Ratio [%]

Soft Story (Y/N)

Vertical Irregularities (Y/N)

Captive Columns (Y/N)

Discontinuity (Y/N)

Signs of Dominant Torsion (Y/N)

Corner Building (Y/N)

Flat Slab (Y/N)

Waffle Slab -Reticular- (Y/N)

Tie Spacing [cm]

Hook Type [deg]

Repair (Y/N)

Splice Failure (Y/N)

Crushing (Y/N)

Bar Buckling (Y/N)

Pounding (Y/N)

Shear Failure (Y/N)

Joint Failure (Y/N)

NS/Street Parallel Masonry Damage

EW/Street Perpendicular Masonry Damage

NS/Street Parallel RC Damage

EW/Street Perpendicular RC Damage

Comments

Report(s)

Photos, Videos, Media.

Drawings/Diagrams

The damage classifications used were:

Buildings in which at least one floor or part of the floor lost its elevation were classified as “collapses”. Damage to buildings with at least one structural failure that rendered the structural element defunct was classified as “severe damage.” Buildings without failures but with crack widths in structural elements exceeding 0.13 mm (0.005 in.) or structural elements with spalling of concrete were classified as having “moderate damage”, and buildings with hairline cracks not exceeding 0.13 mm were rated as having “light damage.” Damage to masonry infill walls was also classified as “severe”, “moderate” or “light.” Damage to masonry walls was rated as “severe” if collapse or see-through cracks were observed. Large cracks in masonry walls and flaking of large pieces of plaster were rated as “moderate damage”, and hairline cracks in masonry walls were classified as “light damage.”

## **APPENDIX B**

Information collected in survey by CICM and SMIE:

<https://www.sismosmexico.org/informes>

Address

Postal Code

Longitude

Latitude

Number of Floors above Ground

Number of Basements

Total Collapse

Partial Collapse

Differential Settlement

Inclination

Structural Damage

Damage to Nonstructural Elements

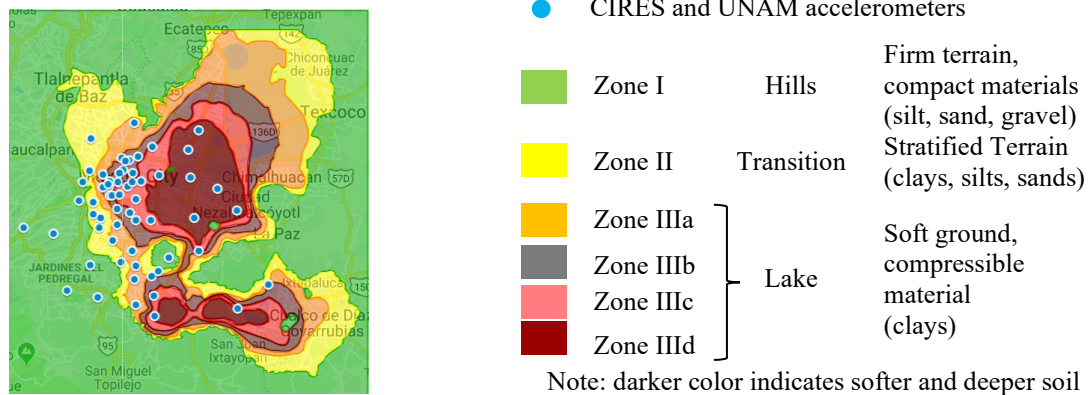
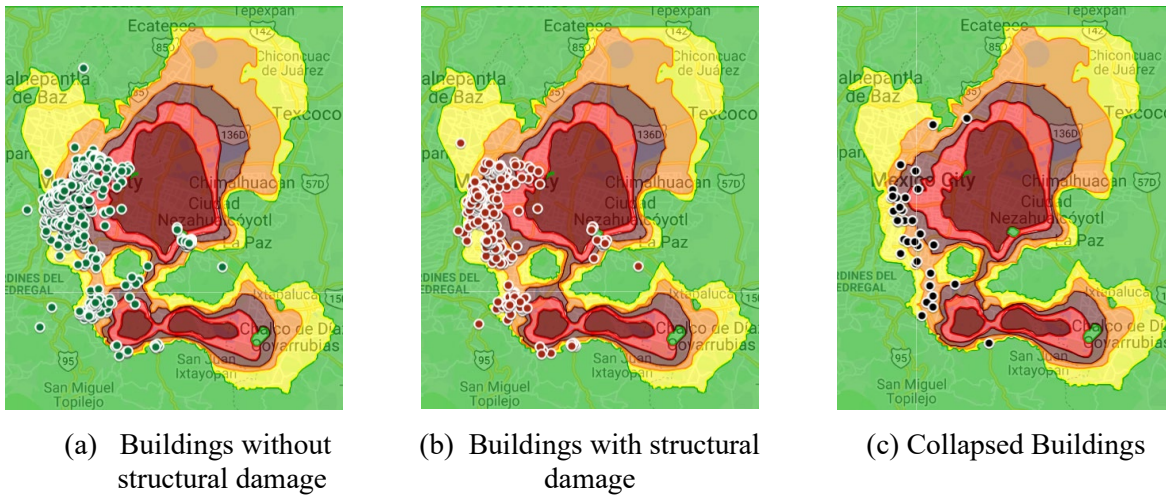


**Figure 1.** Locations of buildings surveyed by CICM and SMIE and CIRES accelerometers superimposed on maps of geotechnical zones (CICM and SMIE, 2017) [COLOR]



**Figure 2.** Examples of collapses in buildings surveyed by CICM and SMIE (2017) [COLOR]



**Figure 3.** Examples of structural damage in buildings surveyed by CICM and SMIE (2017)  
 (COLOR)

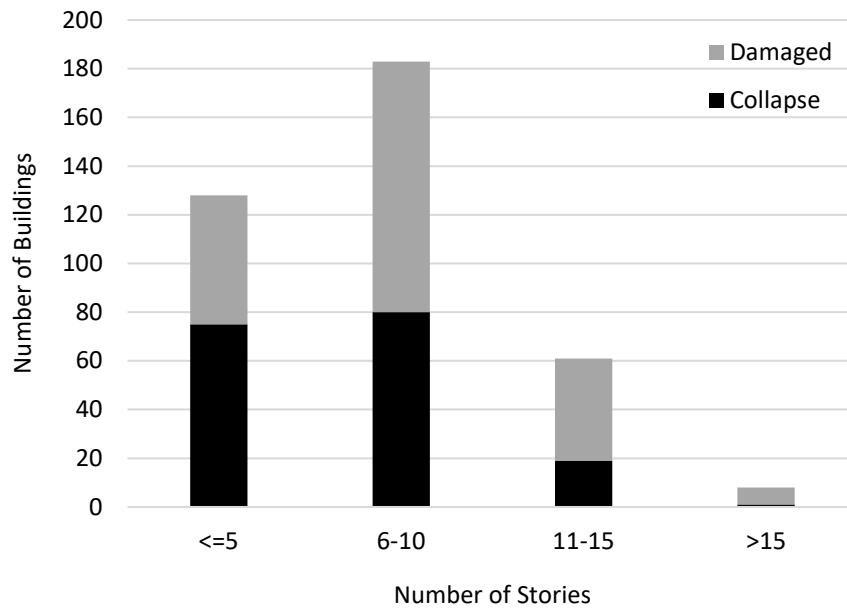
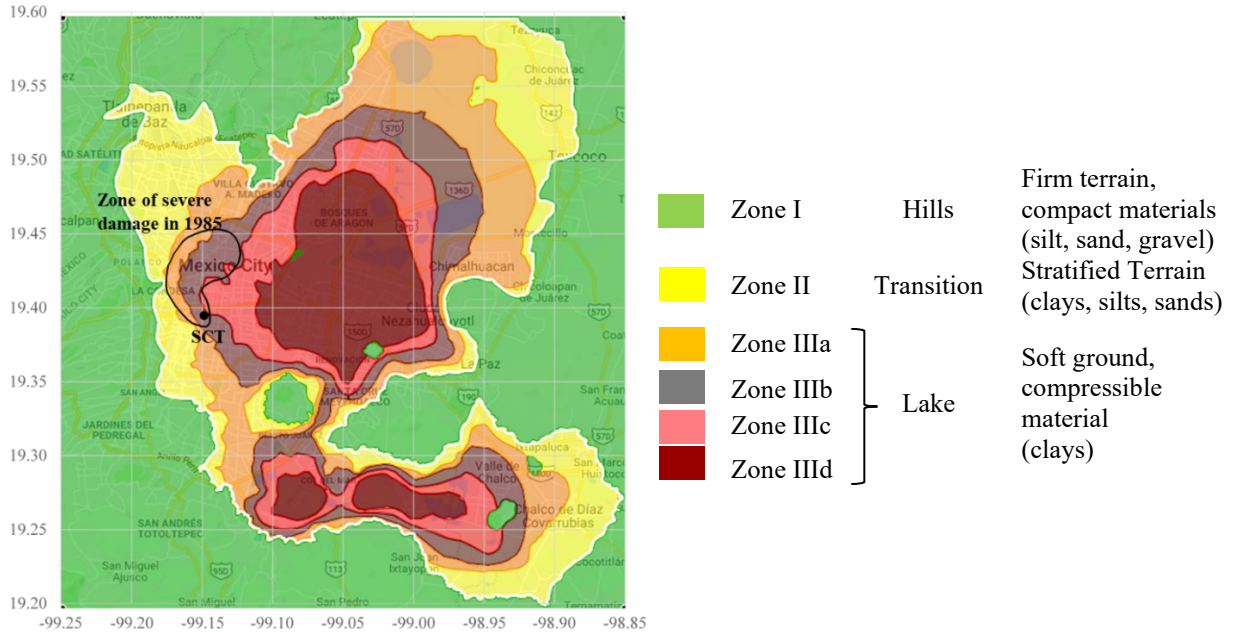
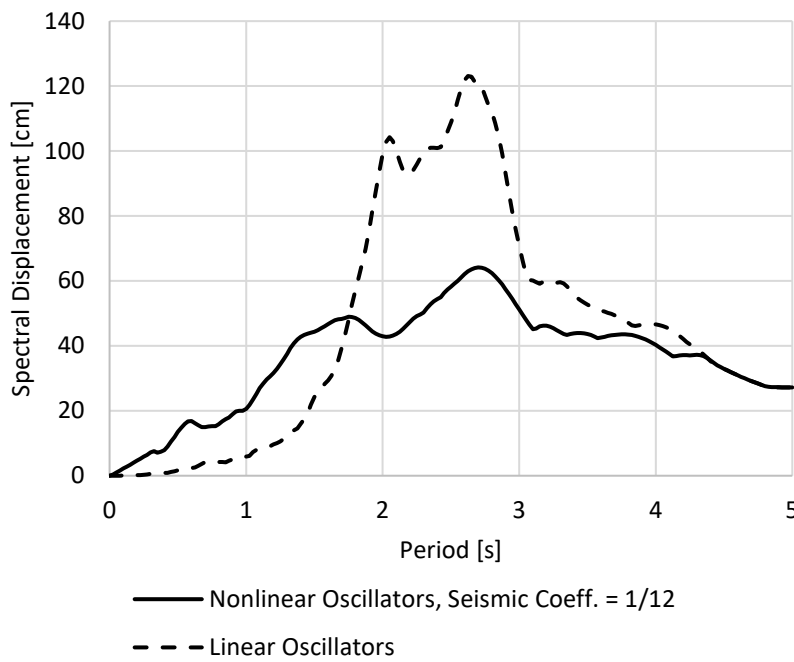


**Figure 4.** Reinforced concrete buildings with severe structural damage and partial or complete collapse, Mexico City, 1985 (Reproduced using data from Aguilar et al. 1989)



(a)



Note:

‘Linear oscillator’ refers to a linear-elastic SDOF spring-mass system which remains in its linear range of response and has a damping ratio of 5%.

Non-linear oscillator, seismic coefficient = 1/12 refers to nonlinear SDOFs with a base shear coefficient (ratio of base shear strength to building weight) of 1/12.

(b)

**Figure 5.** (a) Location of station SCT and zone of severe damage in 1985 (using data from Stone et al 1987), and (b) displacement spectra for SDOF linear and nonlinear oscillators to the E-W component of the 1985 earthquake recorded at the SCT station (damping ratio = 5%). (COLOR)

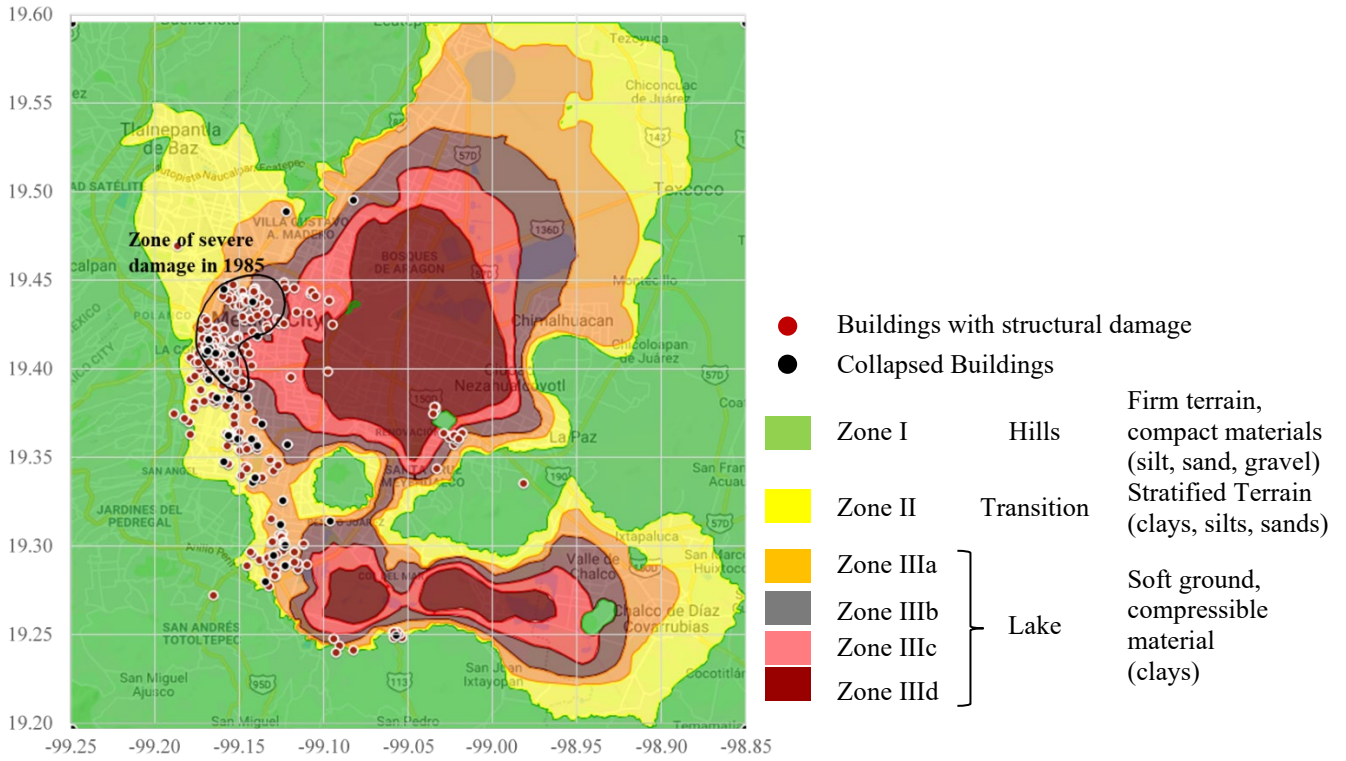


**Figure 6.** Locations of damaged and collapsed buildings after 2017 Puebla-Morelos Earthquake

(COLOR)

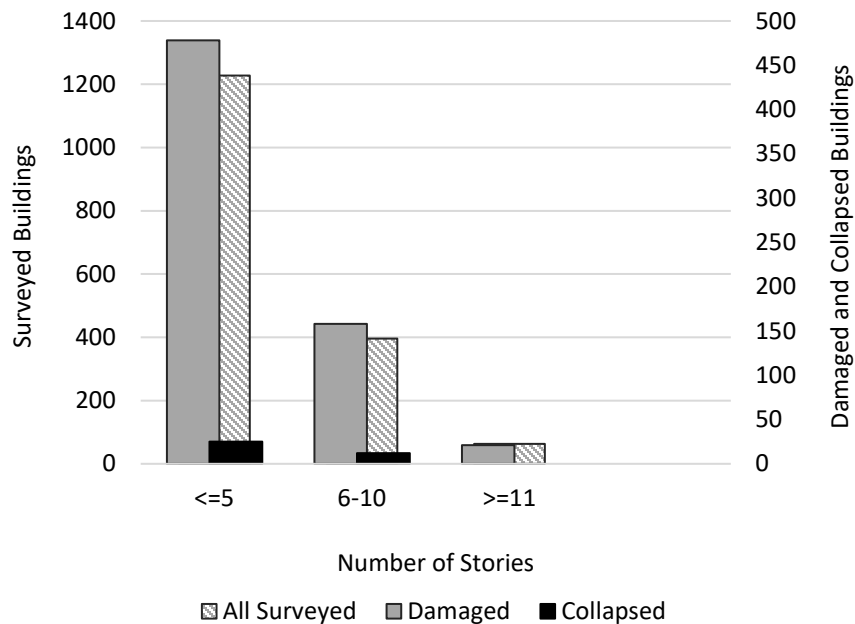


**Figure 7.** Buildings surveyed after 2017 Puebla-Morelos Earthquake (data from CICM and SMIE, 2017) – Note the use of two different vertical scales.

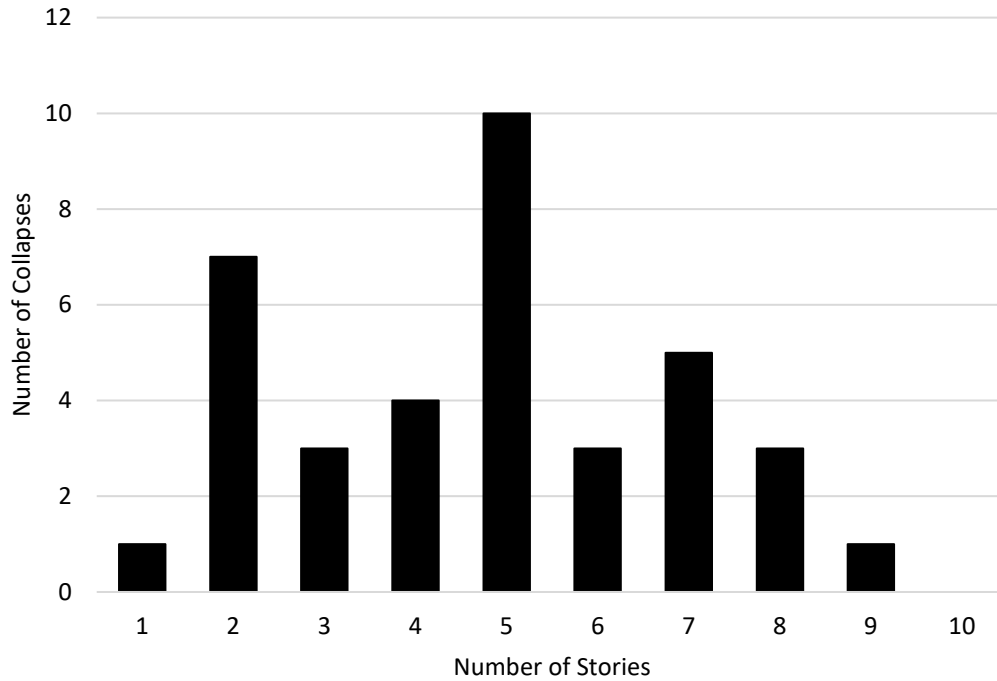


**Figure 8.** Height, in terms of number of stories, of collapsed buildings in Mexico City, 2017  
Puebla-Morelos Earthquake

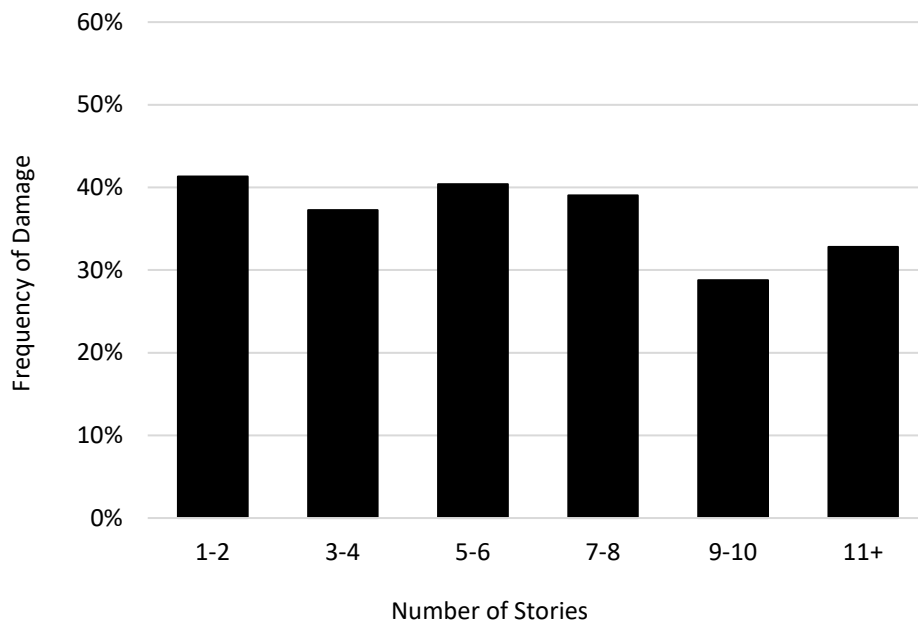


**Figure 9.** Frequency of damage vs. number of stories in 2017

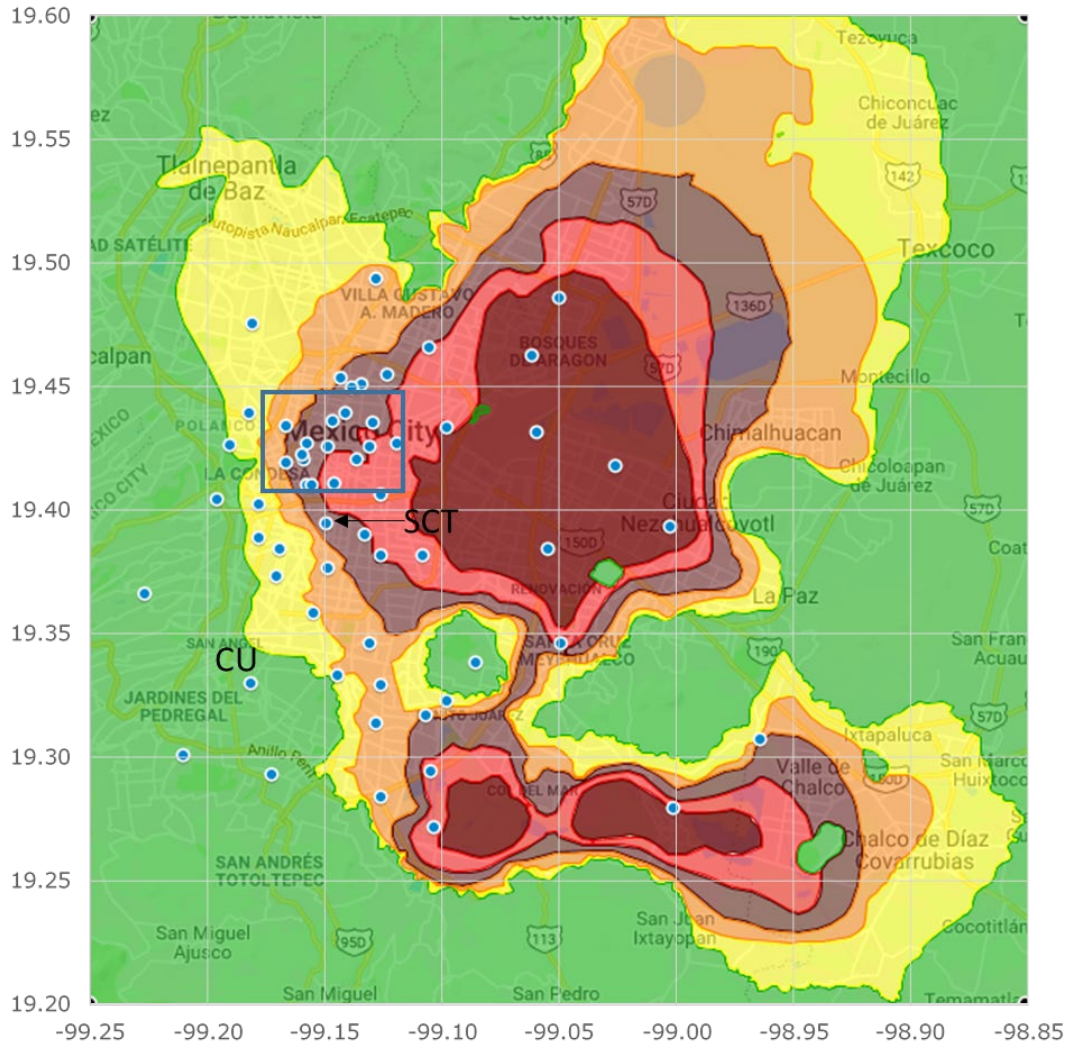
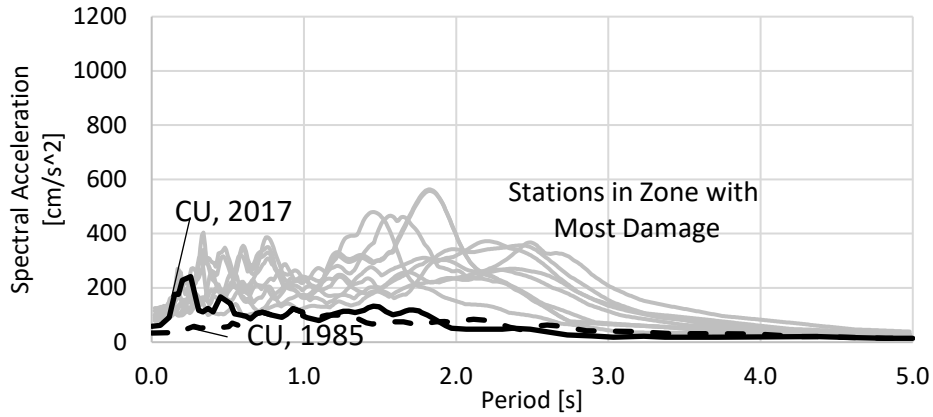
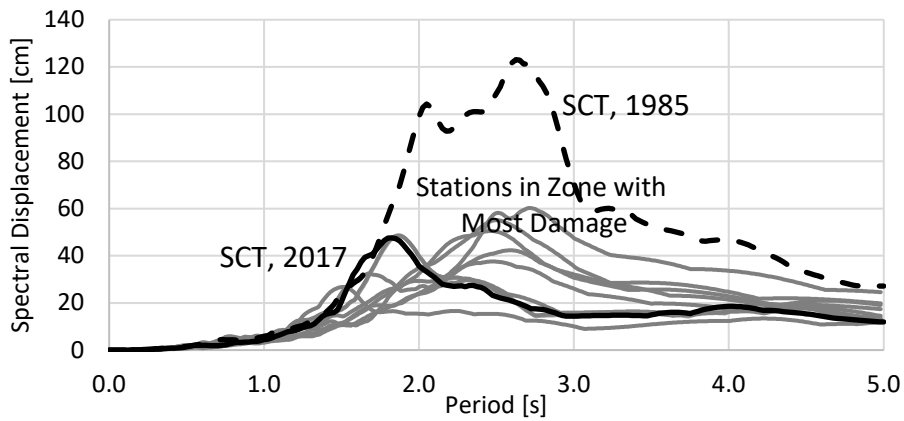


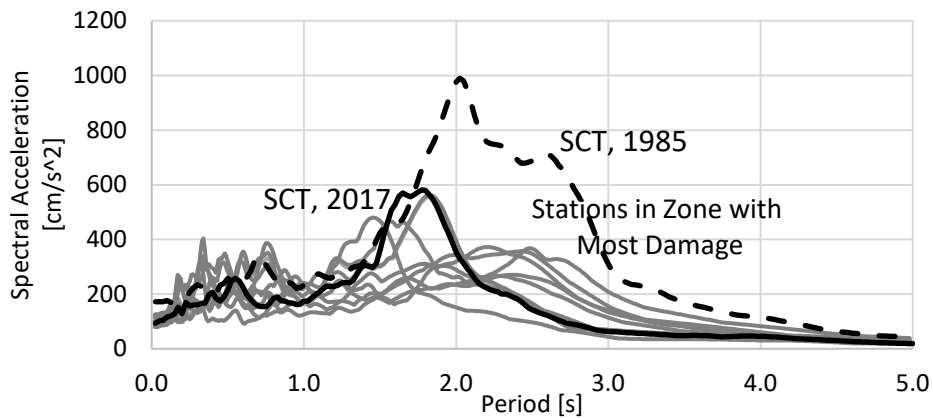
**Figure 10.** Locations of CIRES and UNAM accelerometers in Mexico City (2017) (COLOR)



(a) Station at Ciudad Universitaria (CU), spectral accelerations



(b) Station SCT, spectral displacements



(c) Station SCT, spectral accelerations

**Figure 11.** Spectral displacements and accelerations for the 1985 and 2017 ground motion records (damping ratio = 5%)

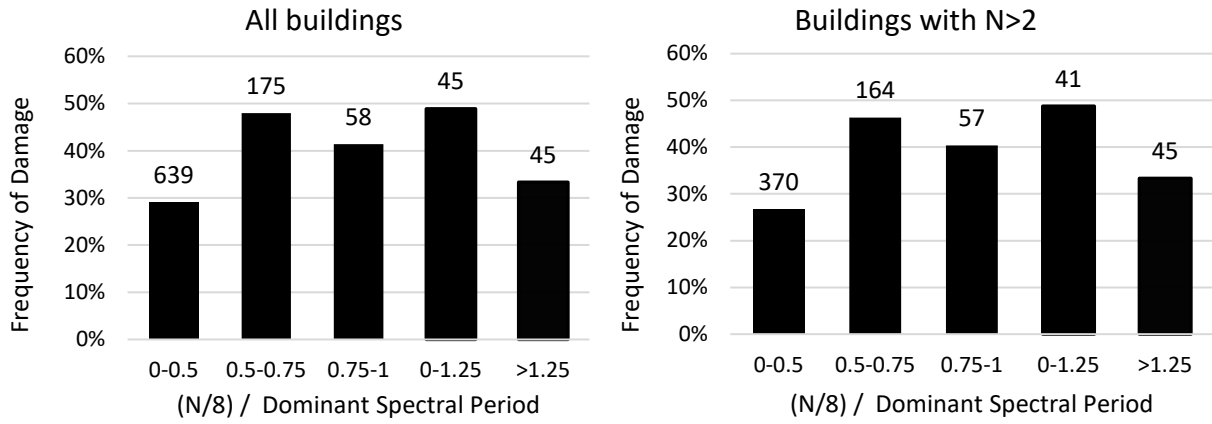
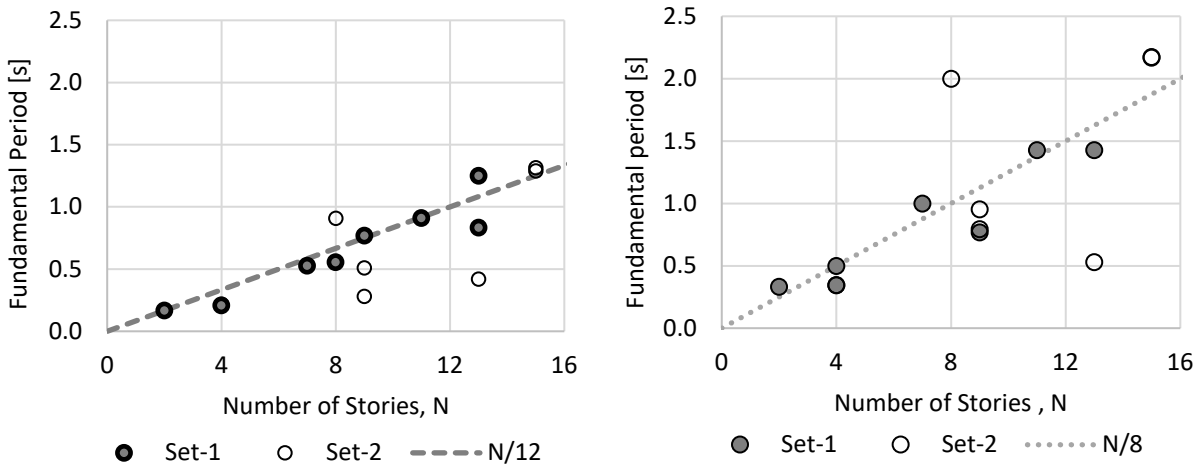


**Figure 12.** Correlation between frequency of damage and dominant spectral period for all buildings (left) and buildings with  $N > 2$  (right)



(a) Strong (perpendicular) direction

(b) Weak (street) direction

**Figure 13.** Longest periods of vibration inferred from ambient vibrations

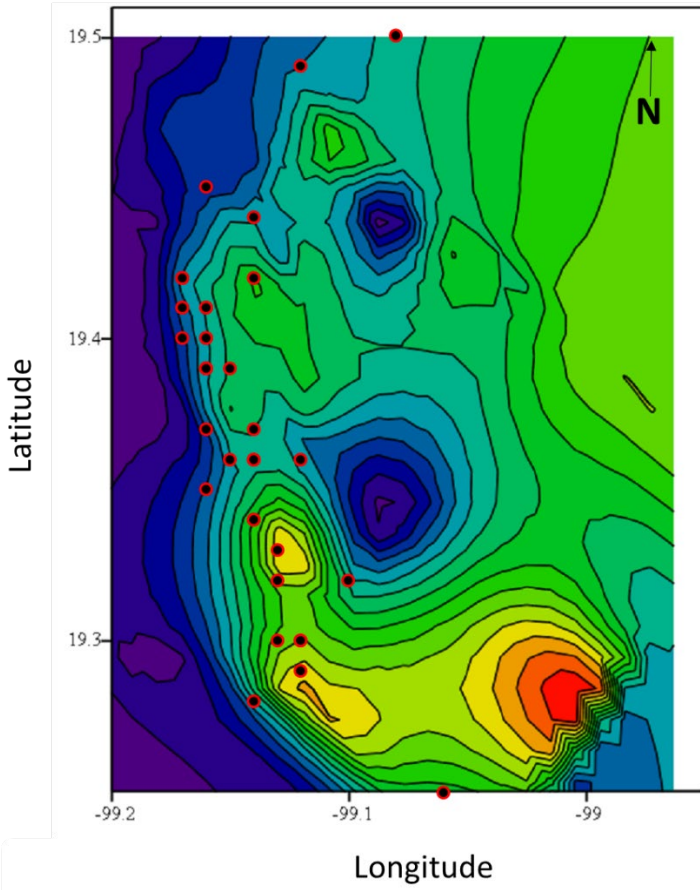


**Figure 14.** Contour of PGV (purple represents low PGV (~10cm/s) and red represents high PGV (~50cm/s), and black dots represent collapsed buildings) (COLOR)

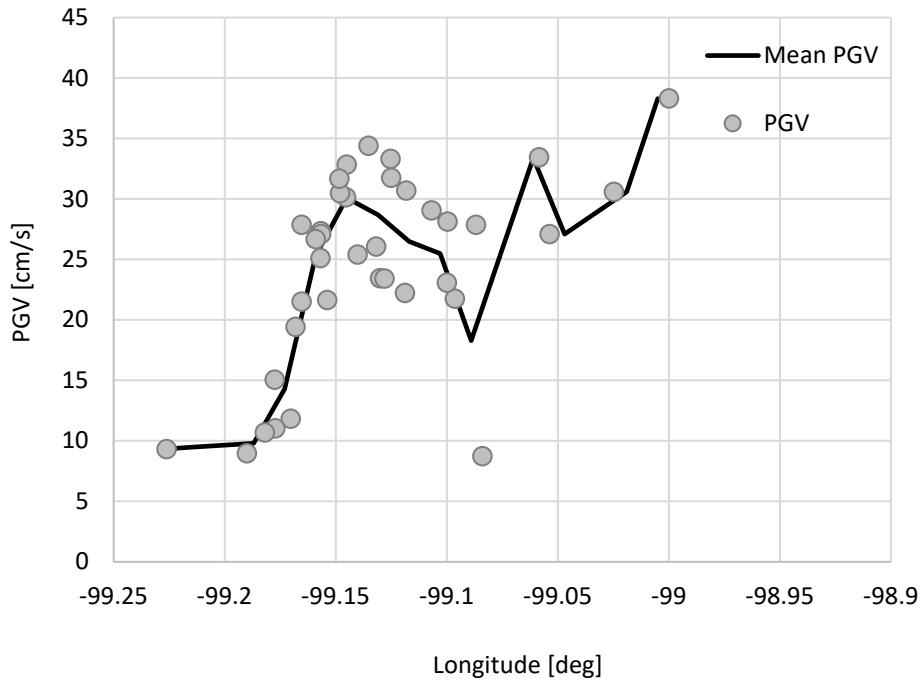


**Figure 15.** Variation of PGV from West to East between latitudes 19.35 and 19.45 degrees

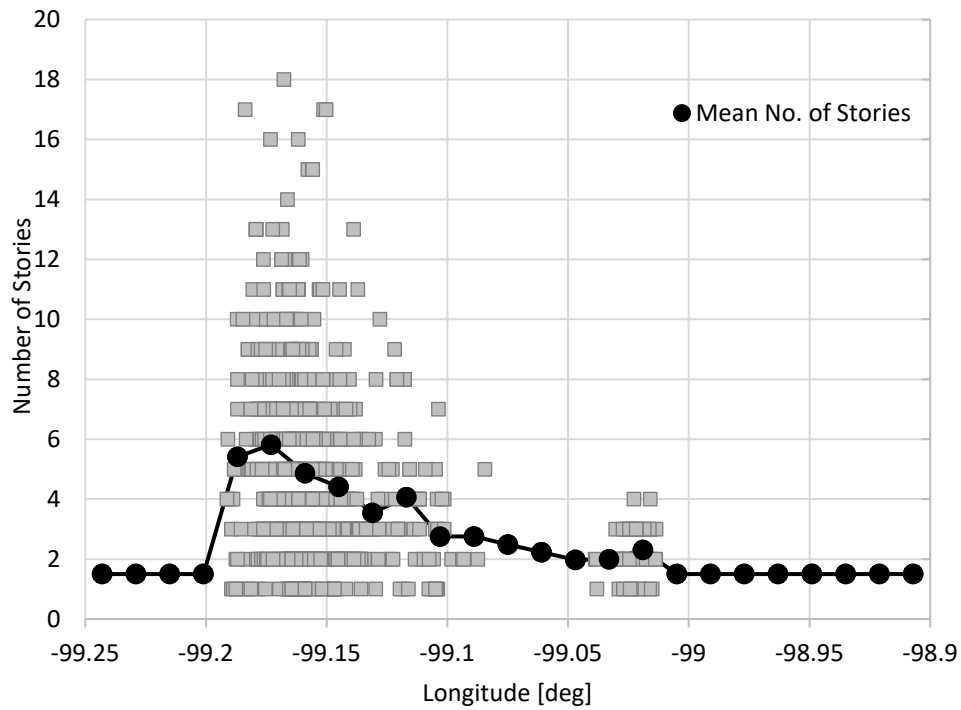


**Figure 16.** Variation of building height from West to East

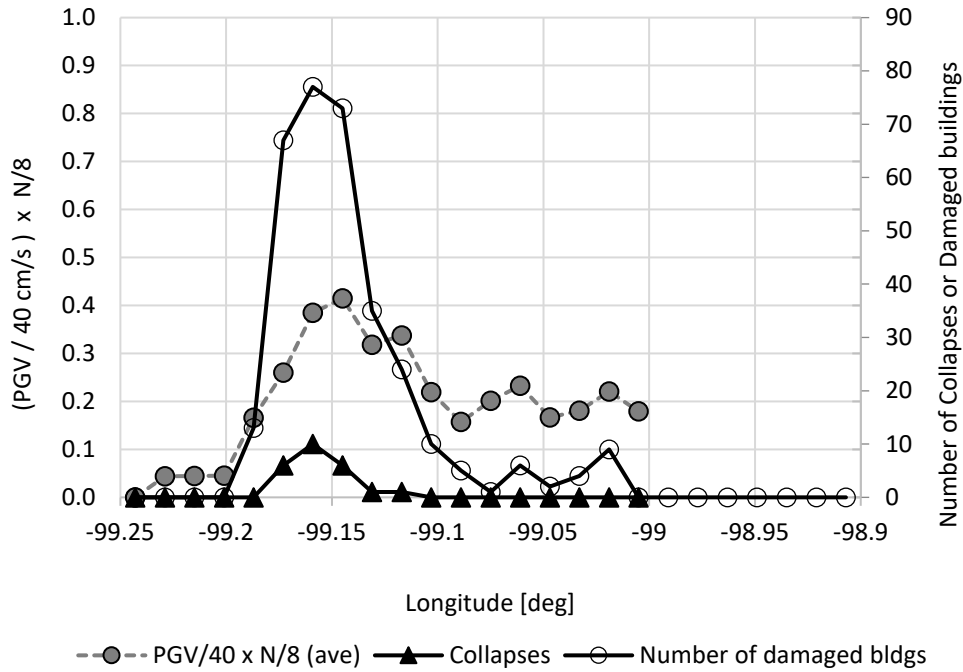


**Figure 17.** Variation of drift demand and collapsed buildings

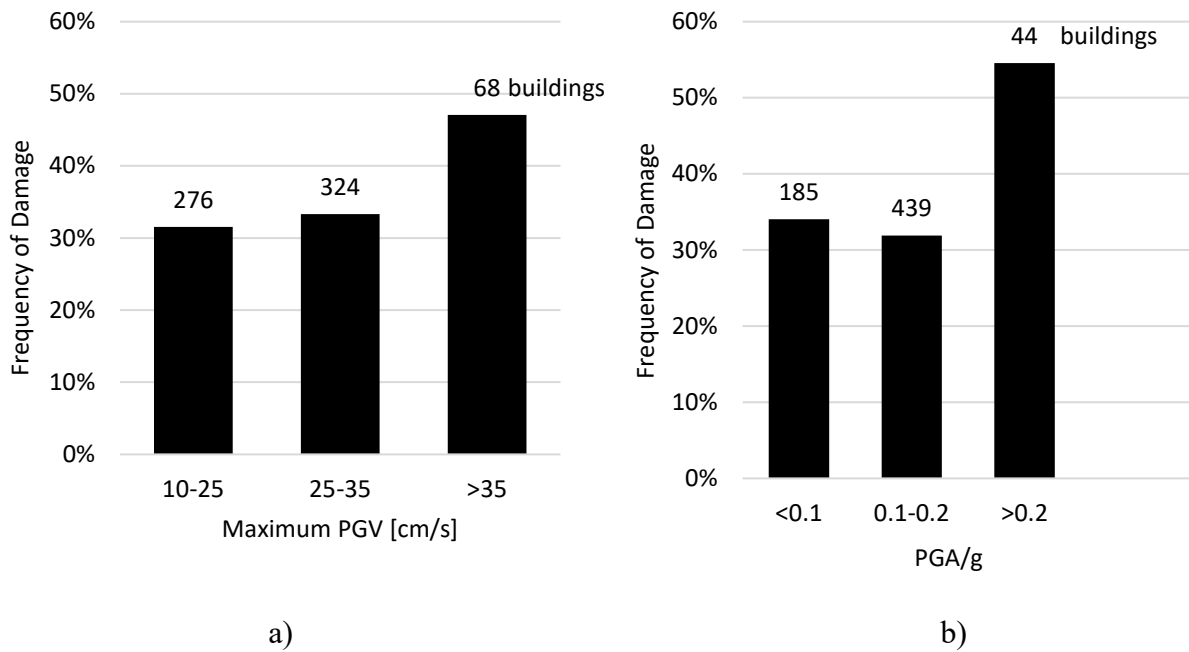


**Figure 18.** Frequency of damage in buildings with  $N > 2$  vs. PGV and PGA

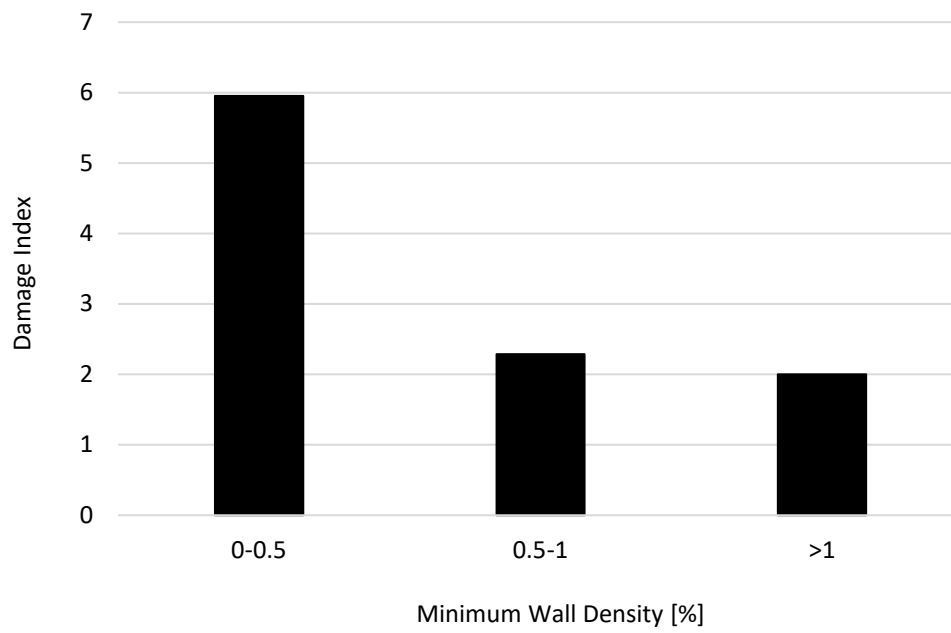


**Figure 19.** Average damage index vs. wall density